

# Fabrication of Highly Uniform Gel Coatings by the Conversion of Surface-Anchored Metal–Organic Frameworks

Manuel Tsotsalas,<sup>†</sup> Jinxuan Liu,<sup>†</sup> Beatrix Tettmann,<sup>†</sup> Sylvain Grosjean,<sup>||,‡</sup> Artak Shahnas,<sup>†</sup> Zhengbang Wang,<sup>†</sup> Carlos Azucena,<sup>†</sup> Matthew Addicoat,<sup>‡</sup> Thomas Heine,<sup>‡</sup> Joerg Lahann,<sup>†</sup> Jörg Overhage,<sup>†</sup> Stefan Bräse,<sup>||,§</sup> Hartmut Gliemann,<sup>†</sup> and Christof Wöll\*,<sup>†</sup>

<sup>†</sup>Institute of Functional Interfaces (IFG), <sup>‡</sup>Soft Matter Synthesis Lab, Institute for Biological Interfaces (IBG), and <sup>§</sup>Institute of Toxicology and Genetics (ITG), Karlsruhe Institute of Technology (KIT), Hermann-von-Helmholtz-Platz 1, 76344 Eggenstein-Leopoldshafen, Germany

<sup>||</sup>Institute for Organic Chemistry (IOC), Karlsruhe Institute of Technology (KIT), Fritz-Haber-Weg 6, 76131 Karlsruhe, Germany

<sup>‡</sup>Jacobs University Bremen, Center for Functional Nanomaterials, 28759 Bremen, Germany

## S Supporting Information

**ABSTRACT:** We report the fabrication of 3D, highly porous, covalently bound polymer films of homogeneous thickness. These surface-bound gels combine the advantages of metal–organic framework (MOF) materials, namely, the enormous flexibility and the large size of the maximum pore structures and, in particular, the possibility to grow them epitaxially on modified substrates, with those of covalently connected gel materials, namely, the absence of metal ions in the deposited material, a robust framework consisting of covalent bonds, and, most importantly, pronounced stability under biological conditions. The conversion of a SURMOF (surface-mounted MOF) yields a surface-grafted gel. These SURGELs can be loaded with bioactive compounds and applied as bioactive coatings and provide a drug-release platform in in vitro cell culture studies.

The potential of metal–organic frameworks, MOFs,<sup>1–3</sup> a porous material constructed from organic linkers and metal or metal-oxo nodes, goes far beyond gas storage and separation, the fields where these coordination polymers (PCPs) first found application. This class of highly porous designer solids is of pronounced interest also for biological and medical applications.<sup>4–7</sup> In the past 15 years, numerous MOF structures have been reported, and in particular, the attachment of functional groups to the organic linkers and to the nodes has provided unique possibilities to confer specific functions to these frameworks. MOFs have had their greatest impact in the fields of catalysis<sup>8–12</sup> and sensing,<sup>13–16</sup> whereas applications in biomedicine are emerging.<sup>17,18</sup> The recent success in increasing the maximum pore diameters to values as high as 10 nm within metal–organic frameworks has been a major breakthrough for life science applications.<sup>19</sup> Pores of this size may allow larger biomolecules, such as small proteins, to be embedded within the framework, thus opening a new dimension for biological and biomedical applications. A recent theoretical analysis of the stability of a particular large-pore MOF type<sup>20</sup> has shown that for this isorecticular series the framework stability is largely provided by direct linker–linker interactions. Because these interactions

scale with the length of the linker, one can predict that the upper limit of pore sizes within MOFs can be extended to at least 20 nm, thus also allowing larger proteins to be accommodated as guests in these lattices.

Surface-mounted MOFs (SURMOFs) grown using liquid-phase epitaxy (LPE) on suitably modified substrates are a particularly interesting class of MOFs with respect to applications in surface coatings, as required, for example, in cell culture experiments. The earliest studies on the suitability of SURMOFs for biological applications revealed major limitations, including the presence of potentially cytotoxic metal ions and the pronounced water instability of the MOF types, which are suited for the SURMOF coating processes.<sup>21</sup> Although a slow degradation of matrix materials may be beneficial for certain medical applications (e.g., in the context of drug release<sup>22</sup>), a marked increase in the water stability of the basic compound would be an important improvement. The same argument applies to the prospect of using MOF coatings for biological (e.g., cell culture substrate)<sup>21</sup> and biomedical (e.g., drug release)<sup>5</sup> applications.

Herein, we present an alternative approach to the fabrication of metal-free, 3D-structured coatings.<sup>23,24</sup> The process to be described here is based on a covalent cross-linking of MOF ligands via copper-free click chemistry<sup>25,26</sup> and yields robust gels with pronounced stability under biological conditions. The surface-grafted gels, SURGELs, obtained by cross-linking the organic struts within a SURMOF combine the advantages of the MOF class of materials with that of a covalently connected gel: they offer enormous variability for introducing functional groups into the framework while featuring a pronounced stability against water and the absence of metal ions. In addition, these SURGEL coatings can be fabricated in the form of well-defined oriented layers with vertical compositional gradients. Our method is based on epitaxially grown metal–organic frameworks<sup>27</sup> deposited on modified substrates using liquid-phase epitaxy (LPE). SURMOFs resulting from this LPE process are crystalline and highly oriented<sup>28</sup> and have a very low defect density.<sup>29</sup> As is the case for bulk MOF materials, SURMOFs can be grown from a large

Received: September 11, 2013

variety of functionalized organic linkers. When using linkers equipped with azide side groups, postsynthetic modifications (PSM) of the frameworks via click chemistry become possible, in bulk MOFs<sup>30</sup> as well as in SURMOFs.<sup>31</sup> Here, we use linkers functionalized with two azide side groups to cross-link the MOFs as described by Ishiwata et al. for bulk (powder) MOF materials.<sup>26</sup>

Figure 1 shows the reaction scheme of bifunctional linker diazido-stilbenedicarboxylic acid (DA-SBDC) and cross-linker

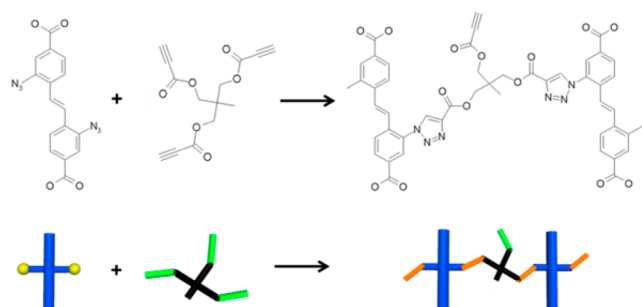


**Figure 1.** Copper-free click reaction between the diazido-stilbenedicarboxylic acid (DA-SBDC) and the cross-linker trimethylolethane tripropiolate and the corresponding schematic representation.

trimethylolethane tripropiolate using a copper-free click reaction and the corresponding schematic representation.

When (DA-SBDC)-SURMOF-2 is immersed in a solution containing an electron-deficient alkyne cross-linker, the spontaneous coupling of alkyne groups with the azido groups in the framework takes place at room temperature.<sup>32</sup> This particular cross-linker contains three alkynyl groups. Because the neighboring electron-withdrawing groups increase the reactivity of the alkyne groups,<sup>33</sup> the alkynyl groups react spontaneously with the azide groups, even in the absence of a catalyst.<sup>25</sup> In previous work, electron-deficient alkyne moieties have found numerous applications, including surface modification, DNA modification, gold nanoparticle functionalization, and hydrogel cross-linking.<sup>25,34–36</sup>

For the experiments carried out in this study, we prepared a (DA-SBDC)-SURMOF-2 grown on COOH-terminated organothiolate surfaces exposed to an organothiolate self-assembled monolayer (SAM). The X-ray diffraction (XRD) data recorded for the SURMOFs (Figure 2) revealed the presence of highly ordered crystalline films, analogous to other variants of the SURMOF-2 reticular class of MOF materials reported in previous work.<sup>20</sup> The observations that the position and relative intensities of the XRD peaks remained virtually unchanged after the cross-linking process demonstrated that the positions of the metal ions contained in the lattice with the largest cross-section<sup>31</sup> were unaffected by the cross-linking process.

The successful coupling reaction was evidenced by the infrared reflection–absorption spectroscopy (IRRAS) data (Figure 2c) where the azido band at 2127  $\text{cm}^{-1}$  from the DA-SBDC linker was substantially decreased after the coupling reaction. (Please note that the  $\text{—C}\equiv\text{C—}$  stretching band of the cross-linker also appears at almost the same position; see Figure S1 for the IRRAS spectrum of the cross-linker.) The appearance of a carbonyl  $\text{C=O}$  stretching band at 1730  $\text{cm}^{-1}$  and a  $\text{C—O—C}$  stretching band at 1250  $\text{cm}^{-1}$  (both assigned to the carbonyl groups contained in the cross-linker, see Supporting Information Figure S1) provided

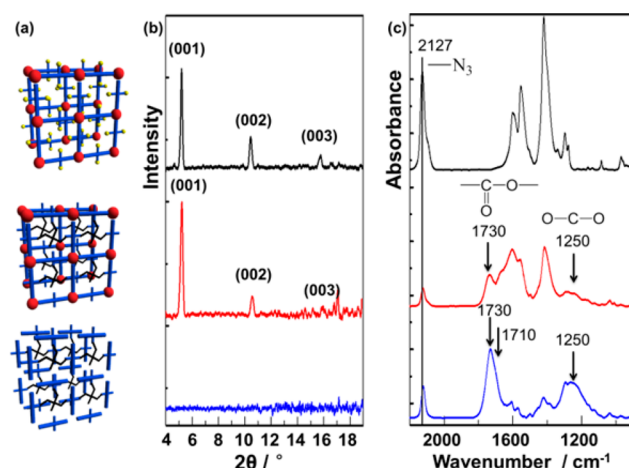


**Figure 2.** (a) Schematic representation of the cross-linking process within the SURMOF-2 structure before the cross-linking reaction (top), after the cross-linking (middle), and after treatment with EDTA for 30 min (bottom). (b) Corresponding X-ray diffraction (XRD) data and (c) IRRAS spectra.

direct evidence of the incorporation of the linker into the SURMOF framework.

To remove the Cu ions from the framework of the cross-linked SURMOF, the substrate was immersed in a solution of ethylenediaminetetraacetic acid (EDTA). As demonstrated in previous work, the SURMOF-2 series is stable with respect to distilled water and artificial seawater<sup>21</sup> but not with respect to solutions containing molecules with a strong coordination affinity for metal ions. The IRRAS spectrum in Figure 2c of pristine SURMOF shows carboxylate bands ( $\text{—COO—}$ , 1610–1550  $\text{cm}^{-1}$  for asymmetric vibration and 1420–1300  $\text{cm}^{-1}$  for symmetric vibration). After immersion of the cross-linked SURMOF for 30 min in EDTA solution, the carboxylate bands mostly disappear (indicating that the carboxylate groups are no longer coordinated to the copper ions), whereas the carbonyl  $\text{C=O}$  stretching band at 1730  $\text{cm}^{-1}$  and the  $\text{C—O—C}$  stretching band at 1250  $\text{cm}^{-1}$  (both assigned to the carbonyl groups contained in the cross-linker) are still present and a shoulder at 1710  $\text{cm}^{-1}$  appears that is assigned to the carbonyl groups contained in the free DA-SBDC linker. (See Supporting Information Figure S1 for the IRRAS spectrum of the free DA-SBDC linker.) As demonstrated, the cross-linked SURMOF shows a pronounced stability against EDTA solution. In contrast, the DA-SBDC SURMOFs without cross-linking showed rapid degradation. After only 5 min, no material was left on the substrate as evidenced by IRRAS (Supporting Information Figure S2).

The presence of an amorphous, surface-grafted film resulting from the removal of the  $\text{Cu}^{2+}$  ions from crystalline MOF was confirmed by the IRRAS and XRD data shown in Figure 2. This data was further supported by energy-dispersive X-ray spectroscopy (EDX) and quartz-crystal microbalance (QCM) data presented in the Supporting Information (Figures S3–S5). Taken together, these analytical methods unambiguously confirmed the presence of a homogeneous, thin gel film on the surface after cross-linking and removal of the metal ions. Moreover, EDX data recorded for the SURMOF-2 films after the cross-linking and after EDTA immersion demonstrated the absence of  $\text{Cu}^{2+}$  ions. As expected, the corresponding XRD data did not show any diffraction signals, thus demonstrating the complete loss of crystallinity. On the basis of these observations,

we concluded that the cross-linked metal–organic framework was converted into an X-ray amorphous polymer gel.

To demonstrate the generality of our approach, we prepared a second, different type of SURGEL based on a layer-pillar-type<sup>37</sup> Cu-DA-SBDC-dabco MOF. XRD patterns and IRRAS spectra recorded for the corresponding SURMOF before and after cross-linking are shown in the Supporting Information (Figures S6 and S7). For both SURMOF variants, the flexibility and length of the three-valent cross-linker was critical because it allowed reactions to take place within a single layer of the SURMOF structures and between neighboring layers. Structural models for these SURMOF structures after the cross-linking are shown in the Supporting Information (Figure S8). The molecular structure and lattice parameters of bare and cross-linked SURMOF bilayers were optimized using a local extension<sup>38</sup> to Rappe's universal force field<sup>39</sup> with the General Utility Lattice Program (GULP), version 4.08.<sup>40,41</sup> The optimized bilayer had lattice constants of  $a = b = 35.3 \text{ \AA}$  and  $c = 5.1 \text{ \AA}$ ; the DA-pillared layered structure had lattice constants of  $a = b = 35.6 \text{ \AA}$  and  $c = 9.1 \text{ \AA}$ . The simulated XRD data for these structures agreed well with the experimental findings (Supporting Information Figures S6 and S9).

A particular advantage of the SURMOF approach is the potential for creating patterned substrates in a straightforward fashion. To this end, a SURMOF was first deposited on a laterally patterned substrate using microcontact printing. The AFM data shown in Figure 3 revealed that the height of the corresponding

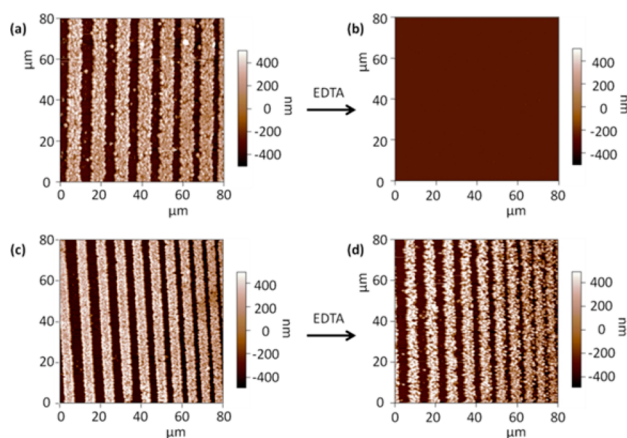


**Figure 3.** AFM analysis of patterned SURMOF samples: (a) pristine sample, (b) pristine sample after EDTA solution, (c) SURMOF after cross-linking, and (d) cross-linked sample after immersion in EDTA solution for 30 min.

SURMOF structures amounted to about 600 nm. The conversion to the interlinked SURMOF and removal of the metal ions using the EDTA solution as described above left the height of the lines unchanged, as demonstrated by the height profiles presented in Figure 3.

These surface-mounted gels, referred to as SURGELS, prepared via cross-linking of a SURMOF precursor layer would also allow the creation of hierarchically structured gels with vertical composition gradients. This type of material has not been accessible via conventional methods but may have a high potential for advanced applications. In particular, the SURGELS offer a promising platform for cell culture experiments.

The huge potential of SURGELS as a substrate for cell culture studies is demonstrated by studying the delivery of biomolecules to the interior of adhering cells. Arabinose, a small sugar, was

used as a prototype biomolecule and loaded into the SURGEL. Subsequently, the substrate was exposed to bacterial cells gene-modified with an arabinose-triggered GFP switch. The induction of GFP expression proved to be highly site-specific; it occurred only for those bacteria in direct contact with the SURGEL substrate.

For these studies, two different types of gene-modified bacteria model organisms, *E. coli* pJN::GFP and *P. putida* pJN::GFP, were used. Both can be considered bacterial model organisms of significant biomedical and biotechnological importance.<sup>42,43</sup> After gene modification, arabinose will induce GFP expression in these microbes in a highly selective manner. The *gfp* gene expression can be detected in a convenient and straightforward fashion by measuring the fluorescence of the synthesized GFP protein.

Figure 4 shows the fluorescence microscopy image after 24 h of incubation of *P. putida* pJN::GFP adhering to the surface of

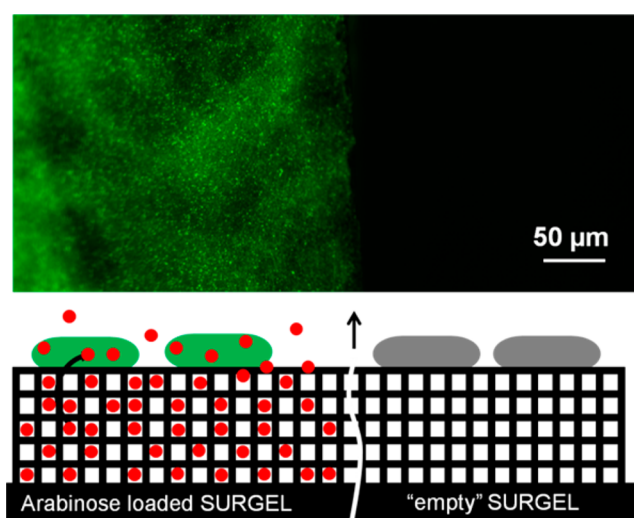


**Figure 4.** Schematic representation and fluorescence microscopy images of *P. putida* pJN::GFP bacteria after 24 h of incubation in the presence of SURGEL substrates. Top: bacteria settled on the SURGEL substrate containing arabinose. Bottom: bacteria settled on an “empty” SURGEL substrate.

arabinose-loaded SURGEL and the corresponding reference SURGEL substrate containing no arabinose. (For these experiments, a pristine SURGEL sample was broken in two and only one of the two pieces was loaded with arabinose. After simultaneous incubation, the two pieces were rejoined for image acquisition.)

For both *E. coli* pJN::GFP and *P. putida* pJN::GFP, the experimental results reveal that only bacterial cells adhering to the surface of arabinose-loaded SURGEL show GFP fluorescence. In contrast, nonadhering bacteria in the broth supernatant and in bacterial cells adhered to SURGEL surfaces without previous arabinose loading showed only marginal GFP fluorescence (fluorescence microscopy images using *E. coli* pJN::GFP and the fluorescence corresponding to the bacteria from the broth supernatant of both bacteria organisms in Supporting Information Figures S10–S12).

These results demonstrate that arabinose-induced *gfp* gene expression is highly localized in space and occurred only at the water/SURGEL interface. We propose that direct contact between the adhering cells and the gel substrate is required for efficient arabinose transport into the bacterial cells. Thus, these



data suggest that SURGELS loaded with bioactive molecules can be used for the specific manipulation of adhering cells. Because SURGELS also offer the possibility of being loaded with different biomolecules and to introduce lateral and vertical compositional gradients, this work opens up a number of applications in biotechnology, including processes such as the biotransformation of surface-attached bacterial biofilms with small chemical compounds or biomedical applications such as spatially localized delivery of high concentrations of bioactive molecules such as antibiotics.

In conclusion, our results demonstrate the successful conversion of a SURMOF into a surface gel, referred to as SURGEL, possessing pronounced stability. This new process to fabricate SURGELS represents a versatile strategy for creating laterally and vertically structured thin films of gel materials with tailorable properties. Further studies to create more complex structures including several vertically organized functional groups are currently ongoing. We also demonstrated the possibility of loading SURGELS with bioactive compounds. Thus, SURGELS loaded with bioactive molecules can be used for the specific manipulation of the cell adhered to the SURGEL surfaces, which can be useful for biotechnological processes such as the biotransformation of substrates or biomedical applications including the spatial delivery of high concentrations of bioactive molecules, including antibiotics.

## ■ ASSOCIATED CONTENT

### Supporting Information

Experimental procedures, computational details, characterization of prepared materials, and details about the biological samples. This material is available free of charge via the Internet at <http://pubs.acs.org>.

## ■ AUTHOR INFORMATION

### Corresponding Author

[christof.woell@kit.edu](mailto:christof.woell@kit.edu)

### Author Contributions

The manuscript was written through the contributions of all authors. All authors have given approval to the final version of the manuscript. Manuel Tsotsalas and Jinxuan Liu contributed equally.

### Notes

The authors declare no competing financial interest.

## ■ REFERENCES

- (1) Alaerts, L.; Kirschhock, C. E. A.; Maes, M.; van der Veen, M. A.; Finsy, V.; Depla, A.; Martens, J. A.; Baron, G. V.; Jacobs, P. A.; Denayer, J. F. M.; De Vos, D. E. *Angew. Chem., Int. Ed.* **2007**, *46*, 4293.
- (2) Chen, B.; Liang, C.; Yang, J.; Contreras, D. S.; Clancy, Y. L.; Lobkovsky, E. B.; Yaghi, O. M.; Dai, S. *Angew. Chem., Int. Ed.* **2006**, *45*, 1390.
- (3) Wang, B.; Cote, A. P.; Furukawa, H.; O'Keeffe, M.; Yaghi, O. M. *Nature* **2008**, *453*, 207.
- (4) Horcajada, P.; Serre, C.; Maurin, G.; Ramsahye, N. A.; Balas, F.; Vallet-Regis, M.; Sebban, M.; Taulelle, F.; Férey, G. *J. Am. Chem. Soc.* **2008**, *130*, 6774.
- (5) Horcajada, P.; Serre, C.; Vallet-Regí, M.; Sebban, M.; Taulelle, F.; Férey, G. *Angew. Chem., Int. Ed.* **2006**, *45*, 5974.
- (6) Huxford, R. C.; Della Rocca, J.; Lin, W. *Curr. Opin. Chem. Biol.* **2010**, *14*, 262.
- (7) McKinlay, A. C.; Morris, R. E.; Horcajada, P.; Férey, G.; Gref, R.; Couvreur, P.; Serre, C. *Angew. Chem., Int. Ed.* **2010**, *49*, 6260.
- (8) Fujita, M.; Kwon, Y. J.; Washizu, S.; Ogura, K. *J. Am. Chem. Soc.* **1994**, *116*, 1151.
- (9) Hasegawa, S.; Horike, S.; Matsuda, R.; Furukawa, S.; Mochizuki, K.; Kinoshita, Y.; Kitagawa, S. *J. Am. Chem. Soc.* **2007**, *129*, 2607.
- (10) Juan-Alcaniz, J.; Ramos-Fernandez, E. V.; Lafont, U.; Gascon, J.; Kapteijn, F. *J. Catal.* **2010**, *269*, 229.
- (11) Lee, J.; Farha, O. K.; Roberts, J.; Scheidt, K. A.; Nguyen, S. T.; Hupp, J. T. *Chem. Soc. Rev.* **2009**, *38*, 1450.
- (12) Ma, L.; Abney, C.; Lin, W. *Chem. Soc. Rev.* **2009**, *38*, 1248.
- (13) Allendorf, M. D.; Bauer, C. A.; Bhakta, R. K.; Houk, R. J. T. *Chem. Soc. Rev.* **2009**, *38*, 1330.
- (14) McManus, G. J.; Perry IV, J. J.; Perry, M.; Wagner, B. D.; Zaworotko, M. J. *J. Am. Chem. Soc.* **2007**, *129*, 9094.
- (15) Stylianou, K. C.; Heck, R.; Chong, S. Y.; Bacsá, J.; Jones, J. T. A.; Khimyak, Y. Z.; Bradshaw, D.; Rosseinsky, M. J. *J. Am. Chem. Soc.* **2013**, *132*, 4119.
- (16) Takashima, Y.; Martinez Martinez, V.; Furukawa, S.; Kondo, M.; Shimomura, S.; Uehara, H.; Nakahama, M.; Sugimoto, K.; Kitagawa, S. *Nat. Commun.* **2011**, *2*, 168.
- (17) Horcajada, P.; Chalati, T.; Serre, C.; Gillet, B.; Sebrie, C.; Baati, T.; Eubank, J. F.; Heurtaux, D.; Clayette, P.; Kreuz, C.; Chang, J.-S.; Hwang, Y. K.; Marsaud, V.; Bories, P.-N.; Cynober, L.; Gil, S.; Férey, G.; Couvreur, P.; Gref, R. *Nat. Mater.* **2010**, *9*, 172.
- (18) Taylor-Pashow, K. M. L.; Rocca, J. D.; Xie, Z.; Tran, S.; Lin, W. J. *Am. Chem. Soc.* **2009**, *131*, 14261.
- (19) Deng, H.; Grunder, S.; Cordova, K. E.; Valente, C.; Furukawa, H.; Hmadeh, M.; Grandara, F.; Whalley, A. C.; Liu, Z.; Asahina, S.; Kazumori, H.; O'Keeffe, M.; Terasaki, O.; Stoddart, J. F.; Yaghi, O. M. *Science* **2012**, *336*, 1018.
- (20) Liu, J.; Lukose, B.; Shekhah, O.; Arslan, H. K.; Weidler, P.; Gliemann, H.; Bräse, S.; Grosjean, S.; Godt, A.; Feng, X.; Müllen, K.; Magdau, I.-B.; Heine, T.; Wöll, C. *Sci. Rep.* **2012**, *2*, 921.
- (21) Hanke, M.; Arslan, H. K.; Bauer, S.; Zybalyo, O.; Christophis, C.; Gliemann, H.; Rosenhahn, A.; Wöll, C. *Langmuir* **2013**, *28*, 6877.
- (22) Mitragotri, S.; Lahann, J. *Adv. Mater.* **2012**, *24*, 3717.
- (23) Li, Q.; Quinn, J. F.; Caruso, F. *Adv. Mater.* **2005**, *17*, 2058.
- (24) Wu, C.; Aslan, S.; Gand, A.; Wolenski, J. S.; Pauthe, E.; Van Tassel, P. R. *Adv. Funct. Mater.* **2013**, *23*, 66.
- (25) Deng, X.; Friedmann, C.; Lahann, J. *Angew. Chem., Int. Ed.* **2011**, *50*, 6522.
- (26) Ishiwata, T.; Furukawa, Y.; Sugikawa, K.; Kokado, K.; Sada, K. *J. Am. Chem. Soc.* **2013**, *135*, 5427.
- (27) Shekhah, O.; Wang, H.; Kowarik, S.; Schreiber, F.; Paulus, M.; Tolan, M.; Sternemann, C.; Evers, F.; Zacher, D.; Fischer, R. A.; Wöll, C. *J. Am. Chem. Soc.* **2007**, *129*, 15118.
- (28) Shekhah, O.; Liu, J.; Fischer, R. A.; Wöll, C. *Chem. Soc. Rev.* **2011**, *40*, 1081.
- (29) Dragasser, A.; Shekhah, O.; Zybalyo, O.; Shen, C.; Buck, M.; Wöll, C.; Schlottwein, D. *Chem. Commun.* **2011**, *48*, 663.
- (30) Wang, Z.; Cohen, S. M. *Chem. Soc. Rev.* **2009**, *38*, 1315.
- (31) Shekhah, O.; Arslan, H. K.; Chen, K.; Schmittl, M.; Maul, R.; Wenzel, W.; Wöll, C. *Chem. Commun.* **2011**, *47*, 11210.
- (32) Rostovtsev, V. V.; Green, L. G.; Fokin, V. V.; Sharpless, K. B. *Angew. Chem., Int. Ed.* **2002**, *41*, 2596.
- (33) Inglis, A. J.; Barner-Kowollik, C. *Macromol. Rapid Commun.* **2010**, *31*, 1247.
- (34) Clark, M.; Kiser, P. *Polym. Int.* **2009**, *58*, 1190.
- (35) Li, Z.; Seo, T. S.; Ju, J. *Tetrahedron Lett.* **2004**, *45*, 3143.
- (36) Limapichat, W.; Basu, A. J. *Colloid Interface Sci.* **2008**, *318*, 140.
- (37) Kitagawa, S.; Kitaura, R.; Noro, S.-i. *Angew. Chem., Int. Ed.* **2004**, *43*, 2334.
- (38) Akter, I. F.; Vankova, N.; Addicoat, M. A.; Heine, T. Manuscript in preparation.
- (39) Rappe, A. K.; Casewit, C. J.; Colwell, K. S.; Goddard, W. A.; Skiff, W. M. *J. Am. Chem. Soc.* **1992**, *114*, 10024.
- (40) Gale, J. D. *Z. Kristallogr. - Cryst. Mater.* **2005**, *220*, 552.
- (41) Gale, J. D.; Rohl, A. L. *Mol. Simul.* **2003**, *29*, 291.
- (42) Alteri, C. J.; Mobley, H. L. T. *Curr. Opin. Microbiol.* **2012**, *15*, 3.
- (43) Poblete-Castro, I.; Becker, J.; Dohnt, K.; Santos, V.; Wittmann, C. *Appl. Microbiol. Biotechnol.* **2012**, *93*, 2279.